ELSEVIER

www.elsevier.nl/locate/jorganchem

Journal of Organometallic Chemistry 596 (2000) 84–89

Journal of Organometallic Chemistry

Structures and properties of complexes $[MCl(C_5Me_5)(N \wedge S)](PF_6)$, M = Rh, Ir, with N ^ S = 1-methyl-2-(alkylthiomethyl)-1*H*-benzimidazole ligands

Markus Albrecht, Thomas Scheiring, Torsten Sixt, Wolfgang Kaim *

Institut für Anorganische Chemie, Universität Stuttgart, Pfaffenwaldring 55, D-70550 Stuttgart, Germany

Received 8 July 1999

Dedicated to Professor F.A. Cotton on the occasion of his 70th birthday.

Abstract

The four complexes $[MCl(C_5Me_5)(N \wedge S)](PF_6)$, M = Rh, Ir; N ^ S = 1-methyl-2-(methylthiomethyl)-1*H*-benzimidazole (mmb) and 1-methyl-2-(*tert*-butylthiomethyl)-1*H*-benzimidazole (mtb) were synthesized and characterized by spectroscopy, electrochemistry and X-ray crystallography (as methanol solvates). The essential coordination features, viz., longer M–S (ca. 2.38 Å) and shorter M–N bonds (ca. 2.09 Å) in five-membered chelate rings are common to all four species. Cyclic voltammetry reveals irreversible two-electron reduction to M^I complexes and partially reversible oxidation to Ir^{IV} species for $[IrCl(C_5Me_5)(mtb)]^+$. The results are discussed in comparison with those obtained for α-diimine (N ^ N) complexes of the $[MCl(C_5Me_5)]^+$ fragments. © 2000 Elsevier Science S.A. All rights reserved.

Keywords: Electrochemistry; Iridium; Rhodium; Structure; Thioethers

1. Introduction

1-Methyl-2-(alkylthiomethyl)-1*H*-benzimidazole ligands have been recently used by us in copper chemistry [1–3] to effect a remarkable valence tautomerism (Eq. (1)), which bears some resemblance to physiologically essential phenomena in amine oxidase enzymes [4–6].

$$LCu^{II}(Q^{2-}) \rightleftharpoons LCu^{I}(Q^{\bullet -}) \quad (1)$$

Q = substituted *o*-quinone

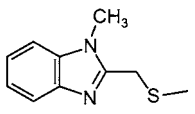

mmb

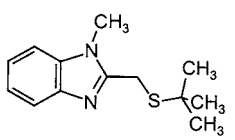

mtb

Mimicking one histidine and one methionine binding site, the neutral 1-methyl-2-(alkylthiomethyl)-1*H*-benzimidazole ligands can form partially saturated (non-conjugated) and thus non-planar five-membered chelates with metal centres.

The (benz)imidazole N and thioether S donor atoms are both weakly π accepting but of different 'softness', so that both copper(I) and copper(II) complexes can form; crystal structures of $[(\eta^2\text{-mmb})Cu(PPh_3)_2](BF_4)$ and $[(\eta^2\text{-mmb})_2Cu(\eta^1\text{-}ClO_4)](ClO_4)$, mmb = 1-methyl-2-(methylthiomethyl)-1*H*-benzimidazole, were recently reported [2], exhibiting essentially similar Cu–S bond lengths for both oxidation states of copper. In order to expand the scope of these simple but hitherto unused [3] ligands, we now describe the synthesis, spectroscopy and structure of the complexes $[MCl(C_5Me_5)(N \wedge S)](PF_6)$ with M = Rh or Ir and N ^ S = mmb (complexes **1** and **2**) or 1-methyl-2-(*tert*-butylthiomethyl)-1*H*-benzimidazole (mtb; complexes **3** and **4**). We also present electrochemical and spectroscopic properties of these systems because complexes of the organometallic $[MCl(C_5Me_5)]^+$ fragments with α-diimines and related unsaturated ligands show a particular electrochemical

* Corresponding author.

PII: S0022-328X(99)00544-6

behaviour [7–10] which has been used for hydride transfer catalysis [11,12].

2. Results and discussion

Compounds **1**–**4** were prepared from the metal precursors $[MCl(\mu\text{-}Cl)(C_5Me_5)]_2$ and the N ^ S ligands. The new 1-methyl-2-(*tert*-butylthiomethyl)-1*H*-benzimidazole was obtained by Phillips condensation [13] in analogy to other such ligands (see Section 3) [1,3]. In contrast to the iridium analogues, the rhodium compounds showed evidence of partial dissociation in acetonitrile solution. The compounds were identified by analysis, ^{1}H- and ^{13}C-NMR spectroscopy (Table 1) and X-ray crystal-structure determination of the methanol solvates $[MCl(C_5Me_5)(N \hat{} S)](PF_6)\cdot CH_3OH$. The results are summarized in Tables 2 and 3, Figs. 1–3 illustrate the molecular structures.

The rhodium and iridium complexes **3** and **4** of the mtb ligand form isomorphous crystals; there are no unusual intermolecular interactions in the crystals of compounds $[MCl(C_5Me_5)(N \hat{} S)](PF_6)$. The metals are chelated by the N–S ligands with long [14] M–S (ca. 2.38 Å) and shorter M–N [15] bonds (ca. 2.09 Å), a situation that has similarly been observed for a copper(I) complex $[(\eta^2\text{-mmb})Cu(PPh_3)_2](BF_4)$ although rhodium(III) and iridium(III) are considered 'hard' metal electrophilic centres in comparison with Cu^I. Silver(I) complexes $[Ag(N \hat{} S)_2](PF_6)$ (2.70 and 2.23 Å [16]) and the copper(II) complex $[(\eta^2\text{-mmb})_2Cu(\eta^1\text{-}ClO_4)](ClO_4)$ (2.43 and 1.945 Å [2]) display a different behaviour due to preferential 2 + 2 coordination (Ag^I) or strong Cu^{II}–N bonds. The unsymmetrical five-membered chelate rings in $[MCl(C_5Me_5)(N \hat{} S)](PF_6)$ are non-planar because of partial saturation; bonding to the C_5Me_5 and chloride ligands is as expected. The M–Cl bonds in compounds with the 1-methyl-2-(*tert*-butylthiomethyl)-1*H*-benzimidazole ligand are slightly longer due to the effect of the bulky *tert*-butyl group; on the other hand, corresponding rhodium and iridium systems differ mainly by the slightly longer bonds to the sulfur atoms in the rhodium complexes as an established consequence of the lanthanide contraction (Table 3).

In cyclic voltammetry experiments (Table 4) the compounds exhibit clear differences: complex $[IrCl(C_5Me_5)(mtb)]^+$ exhibits a detectable, partially reversible oxidation from the trivalent (d^6) to the tetravalent state (d^5; Fig. 4), reflecting the established stabilization of higher oxidation states for the heavier homologues within a transition metal group [17]. Fig. 4 illustrates that this oxidation is accompanied by a small amount of detectable chemical reactivity as indicated by an additional signal on the back scan; on the other hand, the reduction is generally irreversible for all

Table 1
NMR data (δ in ppm) of complexes **1**–**4**

^{1}H-NMR

	$C(CH_3)_3$	CH_3(Cp*)	SCH_3	NCH_3	CH_2(A) [c]	CH_2(B) [c]	J_{AB} [Hz]	Imidazole	
1 [a]		1.79	2.22	3.91	4.08	4.43	17.54	7.45–7.62 (m, 4H)	
2 [b]		1.78	2.23	3.92	4.08	4.35	17.26	7.45–7.55 (m, 3H)	7.62-7.66 (m, 1H)
3 [a]	1.34	1.74		3.96	4.12	4.37	18.00	7.42–7.62 (m, 4H)	
4 [b]	1.38	1.73		4.00	4.00	4.38	18.08	7.43–7.54 (m, 3H)	7.61–7.65 (m, 1H)

^{13}C-NMR

								Imidazole			
	CH_3(Cp*)	SCH_3	$C(CH_3)$	NCH_3	CH_2S [d]	$C(CH_3)$	CCH_3(Cp*)	*C*-5,6	*C*-4,7	*C*-3a,7a	*C*-2
1 [a]	9.73	19.58		32.67	36.25		99.23	112.09, 117.80	124.85, 125.31	136.96, 138.75	153.69
2 [b]	9.44	18.61		33.49	37.17		92.66	112.88, 118.55	125.23, 125.77	137.23, 138.59	157.62
3 [a]	9.52		28.34	32.54	30.01	53.13	99.32	111.96, 118.07	124.62, 125,11	136.77, 138.63	155.12
4 [b]	9.23		28.12	33.51	31.51	54.80	93.13	112.90, 118.74	125.14, 125.71	137.03, 138.51	158.97

[a] In CD_2Cl_2.
[b] In CD_3CN.
[c] AB system; all other ^{1}H-NMR resonances singlets.
[d] Assignment based on DEPT 135-spectroscopy.

Table 2
Crystal data for complexes **1**–**4** as methanol solvates

Compound	$[RhCl(C_5Me_5)(mmb)](PF_6)\cdot CH_3OH$ (**1**)	$[IrCl(C_5Me_5)(mmb)](PF_6)\cdot CH_3OH$ (**2**)	$[RhCl(C_5Me_5)(mtb)](PF_6)\cdot CH_3OH$ (**3**)	$[IrCl(C_5Me_5)(mtb)](PF_6)\cdot CH_3OH$ (**4**)
Empirical formula	$C_{21}H_{27}ClF_6N_2OPRS$	$C_{21}H_{27}ClF_6IrN_2OPS$	$C_{24}H_{37}ClF_6N_2OPRS$	$C_{24}H_{33}ClF_6IrN_2OPS$
Crystal colour, form	Red, cuboids	Yellow, blocks	Red, blocks	Yellow, blocks
Formula weight	638.84	728.13	684.95	770.20
Crystal system	Monoclinic	Monoclinic	Monoclinic	Monoclinic
Space group	$P2_1/c$	$P2_1/c$	$P2_1/c$	$P2_1/c$
a (Å)	13.7790(9)	11.9107(13)	8.477(2)	8.5082(13)
b (Å)	13.2513(12)	14.3298(14)	19.416(6)	19.399(3)
c (Å)	15.776(3)	15.4063(14)	17.645(4)	17.663(3)
β (°)	115.542(10)	93.996(10)	96.49(2)	96.459(13)
V (Å^3)	2599.0(5)	2623.1(5)	2885.6(12)	2896.8(8)
Z	4	4	4	4
$D_{Calc.}$ (Mg m^{-3})	1.633	1.844	1.577	1.766
Absorption coefficient (mm^{-1})	0.962	5.392	0.872	4.888
Diffractometer	Siemens P4	Siemens P4	Siemens P3	Siemens P3
$F(000)$	1288	1416	1400	1512
Crystal size (mm)	$0.15\times0.15\times0.15$	$0.4\times0.3\times0.2$	$0.2\times0.1\times0.1$	$0.3\times0.2\times0.2$
θ range (°)	1.64–25.00	1.71–30.00	1.56–25.00	1.56–30.00
Limiting indices	$-15\le h\le19$, $-16\le k\le18$, $-22\le l\le20$	$-16\le h\le16$, $-4\le k\le20$, $-21\le l\le21$	$-11\le h\le11$, $-4\le k\le27$, $-24\le l\le24$	$-4\le h\le11$, $-27\le k\le27$, $-24\le l\le24$
Reflections collected	5679	7976	5425	8938
Independent reflections	4579	7646	5068	8435
R_{int}	0.0312	0.0396	0.0420	0.0543
Data/restraints/parameters	4462/0/297	7375/1/319	5006/0/350	8247/0/334
Goodness-of-fit on F^2 [a]	1.073	1.058	1.080	1.061
Final R indices $[I>2\sigma(I)]$ [b,c]	$R_1=0.0474$, $wR_2=0.1268$	$R_1=0.0518$, $wR_2=0.1225$	$R_1=0.0347$, $wR_2=0.0915$	$R_1=0.0488$, $wR_2=0.1252$
R indices (all data) [b,c]	$R_1=0.0607$, $wR_2=0.1422$	$R_1=0.0727$, $wR_2=0.1355$	$R_1=0.0382$, $wR_2=0.0946$	$R_1=0.0616$, $wR_2=0.1385$
Largest difference peak and hole (e Å^{-3})	1.094 and −0.627	4.772 and −3.114	0.693 and −0.708	2.881 and −2.309

[a] GOF $=\{\Sigma w(|F_o|^2-|F_c|^2)^2/(n-m)\}^{1/2}$; n = number of data; m = number of variables.
[b] $R=(\Sigma\||F_o|-|F_c|\|)/\Sigma|F_o|$.
[c] $R_w=\{\Sigma[w(|F_o|^2-|F_c|^2)^2]/\Sigma[w(F_o^4)]\}^{1/2}$.

complexes due to chloride dissociation [7–10], the iridium complexes exhibiting much more negative peak potential values than the rhodium analogues. Waves for reoxidation of defined M^I species are not observed; the partially saturated N–S ligands used here cannot engage in charge acceptance like the α-diimine ligands N ^ N (Eq. (2)) [7–10].

$$(C_5Me_5)M^I(N\,\hat{}\,N)\leftrightarrow(C_5Me_5)M^{II}(N\,\hat{}\,N^{-I})\leftrightarrow(C_5Me_5)M^{III}(N\,\hat{}\,N^{-II}) \quad (2)$$

Optical absorption spectra reflect the results from cyclic voltammetry (Table 5, Fig. 5). All compounds have long-wavelength transitions around 400 nm, however, the intensities and assignments are different (Fig. 5). Whereas the iridium compounds exhibit a weak shoulder from a Laporte-forbidden d→d (ligand field) transition, probably including triplet absorptions due to the large spin–orbit coupling constant of that 5d ion [18], the rhodium systems exhibit intense, broad ligand-to-metal charge transfer (LMCT) bands, which occur at higher energy (below 350 nm) for the iridium analogues because of the higher lying LUMO (cf. the more negative reduction peak potential). Scheme 1 illustrates the difference between rhodium and iridium systems. The N ^ S ligands absorb only below 300 nm.

Table 3
Selected bond lengths (Å) and angles (°) for complexes **1**–**4** [a]

Compound	**1**	**2**	**3**	**4**
Bond lengths				
M–N(1)	2.103(4)	2.092(5)	2.090(2)	2.084(4)
M–S	2.4080(13)	2.356(2)	2.3973(10)	2.3697(13)
M–Cl	2.3917(13)	2.396(2)	2.4124(10)	2.4112(14)
Bond angles				
N(1)–M–S	80.00(11)	80.3(2)	80.75(7)	80.88(13)
C(9)–S–M	97.4(2)	98.9(2)	97.31(10)	99.75(5)
C(8)–C(9)–S	109.5(3)	109.7(4)	109.3(2)	108.4(4)
C(8)–N(1)–M	119.4(3)	120.2(4)	119.8(2)	119.7(4)

[a] M = Rh for **1** and **3** or Ir for **2** and **4**.

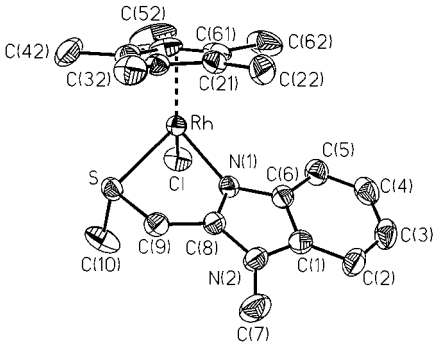

Fig. 1. Molecular structure of the cation in compound **1**.

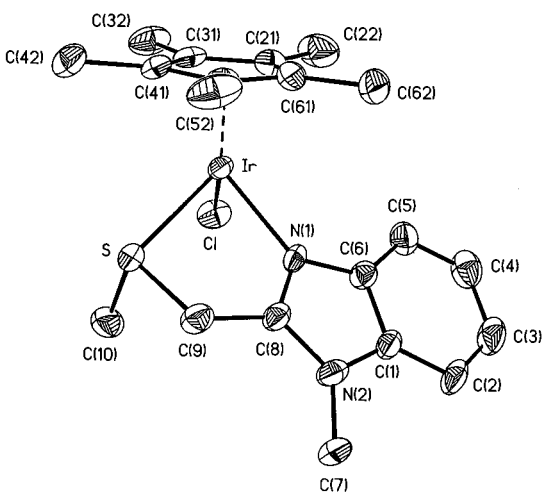

Fig. 2. Molecular structure of the cation in compound **2**.

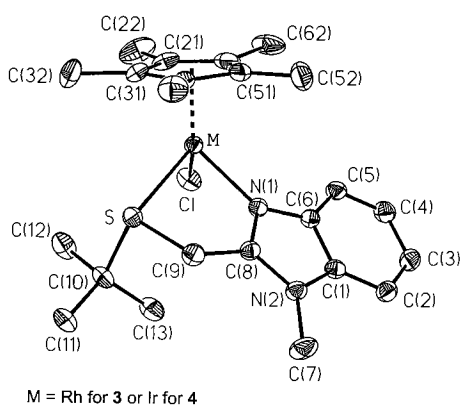

Fig. 3. Molecular structure of the cation in isomorphous compounds **3** and **4** (M = Rh shown).

3. Experimental

3.1. Instrumentation

^{1}H- and ^{13}C-NMR spectra were recorded on a Bruker AC 250 spectrometer and UV–vis absorption spectra on a Bruins Instruments Omega 10 spectrophotometer. Cyclic voltammetry was carried out at 100 mV s^{-1} or higher scan rate in 0.2 M or 0.1 M Bu_4NPF_6 solutions of CH_2Cl_2 or CH_3CN, respectively, using a three-electrode configuration (glassy carbon working electrode, Pt counter electrode, Ag | AgCl reference) and a PAR 273 potentiostat and function generator. The ferrocene–ferrocenium couple served as internal reference.

3.2. Materials

The synthesis of the mmb ligand has been described [1,3]; the 1-methyl-2-(*tert*-butylthiomethyl)-1*H*-benzimidazole can be prepared analogously from *N*-methyl-1,2-phenylenediamine and *tert*-butylmercaptoacetic acid [19] as a sublimable colourless solid. The low yield of that procedure prompted us to follow a different synthetic procedure.

An amount of 2.14 ml (19 mmol) *tert*-butylmercaptan was added slowly to sodium ethanolate prepared by

Table 4
Cyclic voltammetry data for complexes **1**–**4** [a]

Complex	E_{pa}(ox)	E_{pc}(red)
1 [b]	>1.4	−1.38
2 [c]	1.29 [d]	−1.92
3 [b]	>1.4	−1.38
4 [c]	1.30 [e]	−1.94

[a] Anodic or cathodic peak potentials E_p versus $F_c^{+/0}$.
[b] In CH_2Cl_2–0.2 M Bu_4NPF_6.
[c] In CH_3CN–0.1 M Bu_4NPF_6.
[d] Counterpeak at 1.20 V (quasi-reversible wave).
[e] Partially reversible.

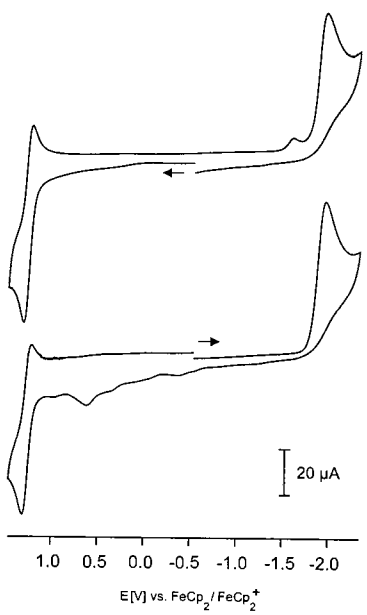

Fig. 4. Cyclic voltammograms for compound **4**, starting with oxidative (top) or reductive scan (bottom); CH_3CN–0.1 M Bu_4NPF_6, 500 mV s^{-1} scan rate.

Table 5
Absorption data of complexes and ligands [a]

1 [c]			388 (2400)	283 (11600)	276 (13600)	269 (13300)
2 [c]		410 [b]	340 [b]	284 (9600)	277 (10500)	271 [b]
3 [c]			396 (2600)	283 (13700)	276 (15500)	268 [b]
4 [c]	410 [b]	355 [b]	318 (1720)	284 (9000)	277 (10000)	270 [b]
mmb [d]			288 (6800)	280 (7700)	274 [b]	258 (7700)
mtb [d]			288 (7500)	280 (8100)	274 [b]	258(8100)

[a] Wavelengths λ_{max} in nm, molar extinction coefficients ε in $dm^3\ mol^{-1}\ cm^{-1}$ (in parentheses).
[b] Shoulder.
[c] In CH_2Cl_2.
[d] In CH_3CN.

reacting 0.44 g (19 mmol) sodium in 30 ml EtOH. To this mixture a solution of 3.43 g (19 mmol) 2-chloromethyl-1-methylbenzimidazole [20,21] in 25 ml ethanol was added. After stirring overnight and removal of the solvent, the residue was washed with water and dried under vacuum. Recrystallization from methanol–water (2:1) and sublimation at 100°C (0.05 Torr) yielded 2.70 g (61%) of 1-methyl-2-(*tert*-butylthiomethyl)-1*H*-benzimidazole. Calc. for $C_{13}H_{18}N_2S$ (234.36): C, 66.62; H, 7.74; N, 11.95. Found: C, 66.64; H, 7.79; N, 11.97%. ^{1}H-NMR (CD_3CN): $\delta = 1.32$ (s, 9H, $C(CH_3)_3$), 3.79 (s, 3H, NCH_3), 4.04 (s, 2H, $CH_2SC(CH_3)_3$, 7.15–7.27 (m, 2H, imidazole), 7.38–7.42 (m, 1H, im.), 7.54–7.58 (m, 1H, im.). ^{13}C-NMR (CD_3CN, assignment based on DEPT 135-spectroscopy): $\delta = 26.23$ ($CH_2SC(CH_3)_3$), 30.89 (NCH_3), 30.93 ($C(CH_3)_3$), 43.93 ($C(CH_3)_3$), 110.56, 119.72 (*C*-5,6 im.), 122.55, 123.16 (*C*-4,7 im.), 137.38, 143.38 (*C*-3a,7a in.), 153.06 (*C*-2 im.).

The complexes $[MCl(C_5Me_5)(N–S)](PF_6)$ were obtained according to the following general procedure (0.1 mmol scale): two equivalents of the appropriate N^S ligand were added to a solution of $[(C_5Me_5)MCl_2]_2$ in methanol. After stirring of the yellow (Ir) or orange (Rh) solutions for 30 min two equivalents of Bu_4NPF_6 were added to precipitate the complexes at 4°C in 60–70% yields. According to the crystal-structure determination the compounds crystallize with one equivalent of methanol. For elemental analyses the air-stable complexes were dried to remove the solvent: Calc. for $C_{20}H_{27}ClF_6N_2PRhS$ (**1**) (610.84): C, 39.33; H, 4.46; N, 4.59. Found: C, 39.25; H, 4.34; N, 4.56%. Calc. for $C_{20}H_{27}ClF_6IrN_2PS$ (2) (700.15): C, 34.31; H, 3.89; N, 4.00. Found: C, 34.33; H, 3.91; N, 3.99%. Calc. for $C_{23}H_{33}ClF_6N_2PRhS$ (**3**) (652.92): C, 42.31; H, 5.09; N, 4.29. Found: C, 42.10; H, 4.69; N, 4.28%. Calc. for $C_{23}H_{33}ClF_6IrN_2PS$ (**4**) (742.23): C, 37.22; H, 4.48; N, 3.77. Found: C, 37.32; H, 4.38; N, 3.60%.

3.3. Crystal-structure analysis

Single crystals were obtained from the reaction mixtures as methanol solvates. For crystal data see Table 2. The structures were solved via direct methods using the SHELXTL-PLUS program package [22]. Refinement was carried out using SHELXL93 [23] employing full-matrix least-squares methods for F^2. All non-hydrogen atoms were refined anisotropically. All H atoms were introduced at idealized positions except for the methanol molecule in **3** (freely refined H). In **2**, the CH_3OH molecule exhibits disorder with respect to the hydroxyl oxygen positions, compound **3** shows a disordered *N*-methyl group.

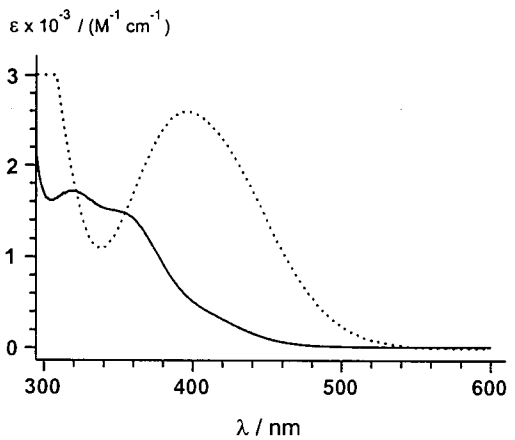

Fig. 5. Absorption spectra of complexes **3** (···) and **4** (—) in CH_2Cl_2.

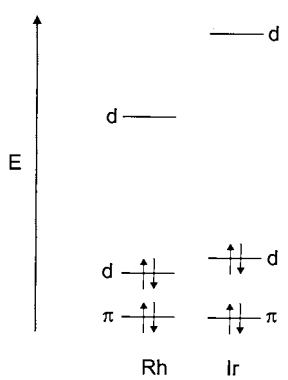

Scheme 1.

4. Supplementary material

Crystallographic data for the structural analysis have been deposited with the Cambridge Crystallographic Data Centre, CCDC nos. 125111–125114. Copies of the information may be obtained free of charge from The Director, CCDC, 12 Union Road, Cambridge, CB2 1EZ, UK (Fax: +44-1223-336033; e-mail: deposit-@ccdc.cam.ac.uk or www: http://www. ccdc. cam.ac.uk).

Acknowledgements

This work was supported by Deutsche Forschungsgemeinschaft (DFG) and the Fonds der Chemischen Industrie. Donations of $RhCl_3$ and $IrCl_3$ from Degussa AG are gratefully acknowledged.

References

[1] J. Rall, E. Waldhör, B. Schwederski, M. Schwach, S. Kohlmann, W. Kaim, in: A.X. Trautwein (Ed.), Bioinorganic Chemistry: Transition Metals in Biology and their Coordination Chemistry, VCH, Weinheim, 1997, p. 476.
[2] M. Albrecht, K. Hübler, T. Scheiring, W. Kaim, Inorg. Chim. Acta 287 (1999) 204.
[3] J. Rall, M. Wanner, M. Albrecht, F.M. Hornung, W. Kaim, Eur. J. Chem. 5 (1999) 2802.
[4] W. Kaim, J. Rall, Angew. Chem. 108 (1996) 47; Angew. Chem. Int. Ed. Engl. 35 (1996) 43.
[5] D.M. Dooley, M.A. McGuirl, D.E. Brown, P.N. Turowski, W.S. McIntire, O.F. Knowles, Nature 349 (1991) 262.
[6] P.N. Turowski, M.A. McGuirl, D.M. Dooley, J. Biol. Chem. 268 (1993) 17680.
[7] M. Ladwig, W. Kaim, J. Organomet. Chem. 419 (1991) 233.
[8] M. Ladwig, W. Kaim, J. Organomet. Chem. 439 (1992) 79.
[9] W. Kaim, R. Reinhardt, E. Waldhör, J. Fiedler, J. Organomet. Chem. 524 (1996) 195.
[10] W. Kaim, S. Berger, S. Greulich, R. Reinhardt, J. Fiedler, J. Organomet. Chem. 582 (1999) 153.
[11] U. Kölle, M. Grätzel, Angew. Chem. 99 (1987) 572; Angew. Chem. Int. Ed. Engl. 26 (1987) 568.
[12] C. Caix, S. Chardon-Noblat, A. Deronzier, R. Ziessel, J. Electroanal. Chem. 403 (1996) 189.
[13] K.A. Williams, J.T. Doi, W.K. Musker, J. Org. Chem. 50 (1985) 4.
[14] (a) A.J. Blake, R.O. Gould, A.J. Holder, T.I. Hyde, M. Schröder, J. Chem. Soc. Dalton Trans. (1988) 1861. (b) A.J. Blake, R.O. Gould, A.J. Holder, T.I. Hyde, G. Reid, M. Schröder, J. Chem. Soc. Dalton Trans. (1990) 1759. (c) K. Brandt, W.S. Sheldrick, J. Chem. Soc. Dalton Trans. (1996) 1237.
[15] (a) R. Krämer, K. Polborn, H. Wanjek, I. Zahn, W. Beck, Chem. Ber. 123 (1990) 767. (b) Y. Zhou, B. Wagner, K. Polborn, K. Stünkel, W. Beck, Z. Naturforsch. 49b (1994) 1193. (c) R. Ziessel, M.-T. Youinou, F. Balegroune, D. Grandjean, J. Organomet. Chem. 441 (1992) 143.
[16] M. Albrecht, K. Hübler, W. Kaim, Z. Anorg. Allg. Chem., in press.
[17] F.A. Cotton, G. Wilkinson, C.A. Murillo, M. Bochmann, Advanced Inorganic Chemistry, 6th ed., Wiley, New York, 1999, p. 878.
[18] A.B.P. Lever, Inorganic Electronic Spectroscopy, 2nd ed., Elsevier, Amsterdam, 1984, p. 478.
[19] A. Mooradian, C.J. Cavallito, A.J. Bergman, E.J. Lawson, C.M. Suter, J. Am. Chem. Soc. 71 (1949) 3372.
[20] C.H. Roeder, A.R. Day, J. Org. Chem. 6 (1941) 25.
[21] A. Bloom, A.R. Day, J. Org. Chem. 4 (1939) 14.
[22] G.M. Sheldrick, SHELXTL-PLUS: An Integrated System for Solving, Refining and Displaying Crystal Structures from Diffraction Data, Siemens Analytical X-ray Instruments Inc., 1989.
[23] G.M. Sheldrick, SHELXL93, Program for Crystal Structure Determination, Universität Göttingen, Germany, 1993.